THE USE OF CHITIN IN THE MOULTS AND EXOSKELETONS OF MEALWORMS (*TENEBRIO MOLITOR*) TO REMOVE CATIONIC DYES FROM AQUEOUS SOLUTIONS

Patrycja Kurowska[1], Tomasz Jóźwiak[1,a,*], Urszula Filipkowska[1,b], Tadeusz Bakuła[2,c]

[1] – Department of Environmental Engineering, University of Warmia and Mazury in Olsztyn, Warszawska 117 Str., 10–720 Olsztyn, Poland
[a] – ORCID: 0000–0003–3360–9827, [b] – ORCID: 0000–0003–0140–6558
[2] – Department of Veterinary Prevention and Feed Hygiene, University of Warmia and Mazury in Olsztyn, Oczapowskiego 13 Str., 10–718 Olsztyn, Poland
[c] – ORCID: 0000–0001–6838–2840
[*]corresponding author: tomasz.jozwiak@uwm.edu.pl

Abstract

We analysed the feasibility of using unmodified chitin exoskeletons and moults of mealworms (Tenebrio molitor) as adsorbents to remove cationic dyes – Basic Violet 10 (BV10) and Basic Red 46 (BR46) – from aqueous solutions. We evaluated the characteristics of the adsorption materials using Fourier-transform infrared spectroscopy and determining the pH of the point of zero charge (pH_{PZC}); the pH effect on dye adsorption effectiveness; dye adsorption kinetics (pseudo–first order, pseudo–second order, and intramolecular diffusion models); and the maximum adsorption capacity of the adsorbents (Langmuir 1 and 2 and Freundlich isotherms). BV10 adsorption on the tested adsorbents was the highest at pH 3, while adsorption of BR46 was highest at pH 6. The adsorption equilibrium time depended mainly on the dye type and its initial concentration; it was 150–210 min for BV10 and 120–150 min for BR46. The maximum adsorption capacity of mealworm exoskeletons reached 5.56 mg/g for BV10 and 31.53 mg/g for BR46, whereas mealworm moults exhibited a higher maximum adsorption capacity, reaching 6.44 mg/g for BV10 and 5.56 mg/g for BR46.

Keywords: *chitin moults, exoskeletons, mealworm, adsorption, cationic dyes*

Received: 07.04.2023
Accepted: 25.05.2023

1. Introduction

The textile, tanning, and paper industries generate wastewater with high concentrations of dyes, which are not very biodegradable due to their complex chemical structure. For this reason, the treatment of coloured industrial wastewater with standard methods based on biological technologies (e.g., activated sludge and biofilm) often proves ineffective [1]. Implementation of ineffective wastewater decolourisation methods by industrial plants may leads to dyes entering the natural environment [2].

The appearance of dyes in natural water bodies is immediately noticeable and very unsightly. A more severe problem, however, is posed by the fact that the dyes dissolved in water limit the access of hydrophytes to sunlight, which impairs primary production. In addition, multiple coloured substances diminish the effectiveness of oxygen diffusion in water, which – when coupled with photosynthesis inhibition – may lead to the development of anaerobic conditions in the aquatic environment [3]. Certain types of cationic dyes may also exert an immediate toxic effect on aquatic organisms. As a consequence, dyes in the aquatic environment may contribute to collapse of the local ecosystem [4]. Hence, it seems advisable to implement the most effective methods for dye removal from wastewater.

Adsorption is one of the most effective and environmentally safe methods for decolourisation of post-production wastewater [5]. In this process, pollutants bind to the surface of adsorbents without producing harmful substances. It is easy to conduct and does not require any expensive or complicated installations. One of the most commonly used adsorbents is activated carbon; however, is relatively expensive and, hence, cheaper alternatives are being sought. One such solution is offered by chitin-based adsorbents. Appropriately pre-treated chitin may prove more effective in dye binding that commercially available activated carbon [6]. This biopolymer is an animal-derived polysaccharide that is the major structural constituent of fungal cell walls and arthropod exoskeletons. Chitin is obtained from crab or shrimp shells in industrial quantities; hence, today, mainly countries with a developed marine shellfish processing industry are able to produce chitin from seafood [7]. The growing market demand for chitin makes it more and more difficult to obtain. In recent years, the insect production industry – for example, mealworms – has begun to develop in many countries for food and feed purposes [8]. Waste from insect breeding includes mainly their moults and exoskeletons. Presumably, in the near future, these materials will represent an alternative source of chitin.

As for crustacean shells, obtaining pure chitin from moults and exoskeletons of insects is time consuming and expensive. In addition, the remaining components of the arthropod skeleton constituting 70%–90% of its original weight, such as proteins and mineral salts, are irretrievably lost in this process [9]. Theoretically, both protein and mineral structures present in the exoskeletons of insects may show some adsorption properties towards dyes. Therefore, demineralisation and deproteinisation of arthropod exoskeletons for the production of chitin adsorbents may turn out to be a waste of time, energy, and adsorption material.

Considering the above, we aimed to examine the effectiveness of adsorbing two popular cationic dyes – Basic Violet 10 (BV10) and Basic Red 46 (BR46) – onto moults and exoskeletons of mealworms (*Tenebrio molitor*).

2. Materials

2.1. Adsorbents: Mealworm Moults (MM) and Mealworm Exoskeletons (ME)

MM and ME were obtained from a laboratory insect culture of the Department of Veterinary Prevention and Feed Hygiene, University of Warmia and Mazury in Olsztyn, Poland. The insects were fed with oat meals and carrots. The chitin content was 8.4%–9.6% for ME and 17.0%–18.0% for MM [10, 11]

2.2. Adsorbates: Dyes

BV10 and BR46 were purchased from the 'BORUTA S.A.' dye production plant in Zgierz (Łódź Voivodeship, Poland). BV10 is a popular cationic dye belonging to the class of xanthene dyes; its cationic nature is due to the presence of a quaternary ammonium cation in its structure. Its characteristic feature is the presence of a carboxyl functional group capable of ionisation and generation of a local negative charge (Figure 1). It is usually used to dye cotton and leather. BR46 is a typical cationic dye belonging to the class of single azo-dyes. Like BV10, it contains a quaternary ammonium cation, which imparts an alkaline character (Figure 1). BR46 is used to dye leather and cotton and as an additive to printing inks and hair dyes.

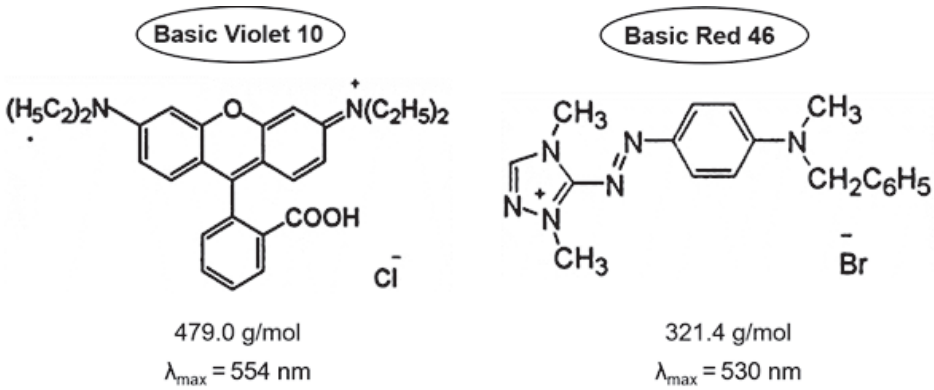

Figure 1. Structures of Basic Violet 10 and Basic Red 46.

2.3. Chemical Reagents

The following chemical reagents were used in the study:

- hydrochloric acid (HCl) 37% (to adjust the pH of solutions);
- sodium hydroxide (NaOH) > 99.9% microgranules (to adjust the pH of solutions); and
- buffer solutions for calibrating the pH meter (pH 4 ± 0.05, pH 7 ± 0.05, and pH 10 ± 0.05).

All chemical reagents used were purchased from POCH S.A. (Poland) and were of p.a. (analytical) purity or higher.

2.4. Laboratory Equipment

The following laboratory equipment was used in the study:

- HI 110 pH meter (HANNA Instruments, Poland) to measure and adjust the pH of solutions;
- MS-53M multi-channel stirrer (JEIO TECH, Korea) for the process of adsorption;

- UV-3100 PC spectrophotometer (VWR, Canada) to determine the concentration of dye in solutions; and
- FT/IR-4700LE Spectrometer with a single reflection attenuated total reflectance attachment (JASCO International, Japan) to generate the adsorbent's Fourier-transform infrared (FTIR) spectra.

3. Methods

3.1. Preparation of Adsorbents from MM and ME

A similar procedure was applied to prepare adsorbents from MM and ME. The material was disintegrated in a laboratory grinder and then sieved through screens with mesh diameters of 3 and 2 mm. The fraction left after the second sieving (2–3 mm in diameter) was washed with deionised water. The washed biomass was then placed in a beaker with petroleum ether for 24 h to allow the wax covering it to dissolve. Then, the biomass was filtered on a laboratory screen (with a mesh diameter of < 0.5 mm) and washed with deionised water until the typical ether odour had disappeared. The material was dried in a laboratory drier (105°C). When dried, the MM and ME was stored in an airtight polyethylene container before use in the adsorption experiments.

3.2. The Effect of pH on Dye Adsorption Effectiveness

First, 0.200 g (dry mass) of MM or ME was weighed using a precise scale to a series of 250-mL beakers. Then, 200 mL of BV10 or BR46 solution (10 mg/l and pH 2–11) was added to each beaker, which was then placed on a multi-station magnetic stirrer set at 200 rpm, which ensured the adsorbent was mixed evenly throughout the solution. After 120 min of adsorption, samples of the solutions were collected from beakers with an automatic pipette (10 ml) to test tubes that had been prepared earlier. The concentration of dye left in the solution after adsorption was determined with a spectrophotometric method. The pH of the solutions after adsorption was also measured.

3.2.1. pH of the Point of Zero Charge (pH_{PZC}) Measurement Using the 'Drift' Method

The pH_{PZC} of the tested adsorbents was measured very similarly to the method described in Section 3.2. Instead of dye solutions with a pH range of 2–11, deionised water with pH adjusted to the pH range of 2–11 was used. After 120 min of mixing the adsorbent in deionised water solutions (pH 2–11), the pH was measured. Then, for each adsorbent, a line chart was generated with the obtained data, where the x-axis is the initial pH and the y-axis is the difference between the final pH and the initial pH ($pH_E - pH_0$). The intersection of the curve with the X axis is the pH_{PZC} of the adsorbent.

3.3. Analyses of Dye Adsorption Kinetics

First, 1.000 g (dry mass) of the adsorbent was weighed into a series of 1000-mL beakers. Then, dye solutions (1000 mL) with the following concentrations were added: 10 and 25 mg/l for BV10 and 25 and 200 mg/l for BR46. The optimal adsorption pH was determined based on the procedure described in Section 3.2. The beakers were placed on a multi-station magnetic stirrer (200 rpm). After specified time intervals (10, 20, 30, 45, 60, 90, 120, 150, 180, 240, and 300 min), samples (2 ml) of solutions were collected for the spectrophotometric determination of the dye concentration.

3.4. Maximum Adsorption Capacity

First, 0.200 g (dry mass) of the adsorbent was weighed and placed into a series of 250-mL beakers. Then, dye solutions (200 mL) with the following concentrations were added: 2–25

mg/l for BV10 and 10–500 mg/l for BR46. The optimal adsorption pH was determined based on the procedure described in Section 3.2. Next, the flasks were placed on a multi-station magnetic stirrer (200 rpm) for the time needed to reach the adsorption equilibrium (established based on the analyses described in Section 3.3). Once the adsorption equilibrium had been reached, the samples were collected for the spectrophotometric analysis of the concentration of the dye left in the solution.

The analyses described in Sections 3.2–3.4 were conducted in three replicates, for each adsorbent and for each dye, at room temperature (20°C). Samples of the solutions collected with an automatic pipette were clear and free of adsorbent particles, so they required filtering before the spectrophotometric determination of the dye concentration. Differences in the concentrations of dyes (Sections 3.3–3.4) were due to their various adsorption effectiveness observed in the preliminary study.

3.5. Calculation Methods

The amount of dye adsorbed on MM or ME was determined from Equation 1:

$$Q_s = \frac{(Co - Cs) \cdot V}{m}, \tag{1}$$

where:

Q_s – mass of the adsorbed dye [mg/g];
C_o – initial concentration of the dye [mg/l];
C_s – concentration of the dye after adsorption [mg/l];
V – volume of the solution [l];
m – adsorbent mass [g].

Experimental data obtained from studies into the kinetics of dye adsorption onto MM/ME were described using the pseudo-first order (Equation 2), pseudo-second order (Equation 3), and intramolecular diffusion (Equation 4) models.

$$Q_s = q_e \cdot (1 - e^{(-k_1 \cdot t)}) \tag{2}$$

$$Q_s = q_e - \frac{q_e}{1 + q_e \cdot k_2 \cdot t} \tag{3}$$

$$Q_s = k_{id} \cdot t^{0.5} \tag{4}$$

where:

Q_s – instantaneous concentration of the adsorbed dye [mg/g];
q_e – the amount of dye adsorbed at equilibrium [mg/g];
t – time of adsorption [min];
k_1 – pseudo-first order adsorption rate constant [1/min];
k_2 – pseudo-second order adsorption rate constant [g/(mg·min)];
k_{id} – intramolecular diffusion model adsorption rate constant [mg/(g·min$^{0.5}$)].

Experimental data obtained from the maximum adsorption capacity experiment were described using the Langmuir 1 (Equation 5), Langmuir 2 (double Langmuir isotherm; Equation 6), and Freundlich (Equation 7) isotherms.

$$Q_s = \frac{Q_{max} \cdot K_c \cdot C}{1 + K_c \cdot C} \quad (5)$$

$$Q_s = \frac{b_1 \cdot K_1 \cdot C}{1 + K_1 \cdot C} + \frac{b_2 \cdot K_2 \cdot C}{1 + K_2 \cdot C} \quad (6)$$

$$Q_s = K \cdot C^n \quad (7)$$

where:
Q_s – mass of the adsorbed dye [mg/g];
C – concentration of the dye left in the solution [mg/l];
Q_{max} – maximum adsorption capacity in the Langmuir model [mg/g];
b_1 – maximum adsorption capacity of the adsorbent (type I active sites) [mg/g];
b_2 – maximum adsorption capacity of the adsorbent (type II active sites) [mg/g];
K_c – constant in the Langmuir model [l/mg];
K_1; K_2 – constants in the Langmuir 2 model [l/mg];
K – the adsorption equilibrium constant in the Freundlich model;
n – constant in the Freundlich model.

4. Results and Discussion

4.1. FTIR Spectra of MM and ME

The spectra of MM and ME are very similar and include bands typical of chitin, proteins, and lipids (Figure 2).

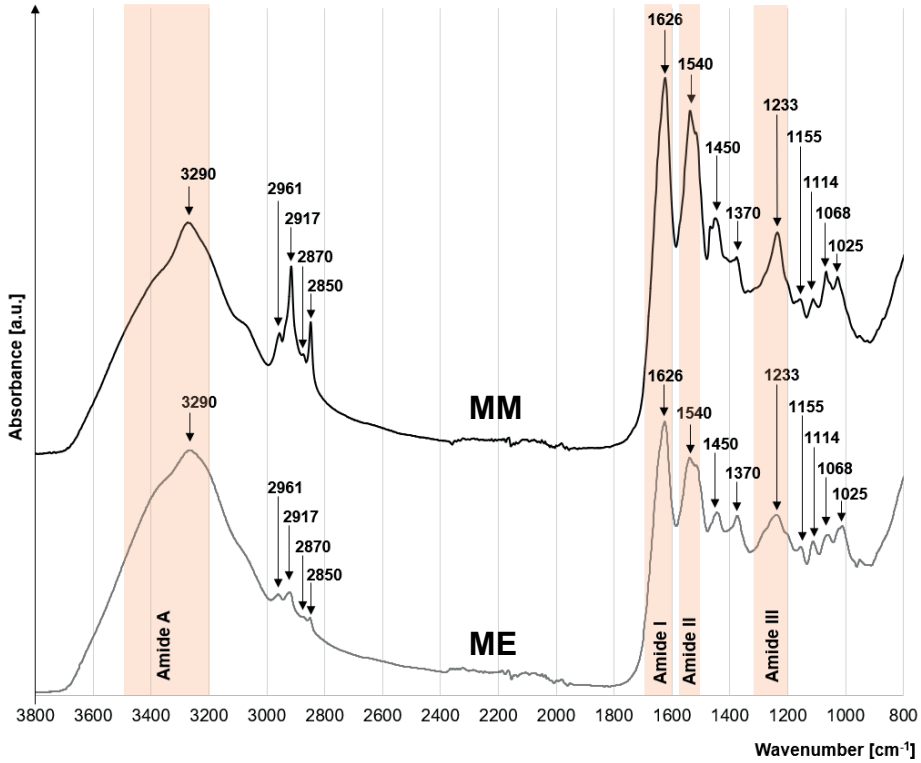

Figure 2. Fourier-transform infrared spectra of mealworm moults (MM) and mealworm exoskeletons (ME).

The peak at 1626 cm^{-1} in the amide I band corresponds to a hydrogen bridge C=O with a hydroxymethyl group of the successive chitin residue of the same chain. In turn, the peak at 1540 cm^{-1} in the amide II band indicates bending of the N–H bond of the acetamide functional group [12, 13]. The presence of acetamide groups in the structure of the tested materials is also confirmed by their characteristic peaks at 3290 and 2870 cm^{-1} corresponding to N–H (amide A) and C=O bonds, respectively [14]. The presence of the C=O bond is also indicated by the peak at 1233 cm^{-1}, which is noticeable in the amide III band [15].

The presence of the saccharide structure in the tested materials, resulting from chitin, is denoted by peaks at 1068 and 1025 cm^{-1} corresponding to the stretching of the C–O bond of C3 carbon and C6 pyranose, respectively [16]. Other characteristic saccharide ring signals are the peaks at 1155 and 1114 cm^{-1} corresponding to the symmetric stretching of the C–O–C bond and asymmetric stretching of the C–O bond, respectively [16]. A small peak at 2961 cm^{-1} points to the presence of the methine group in the pyranose ring [17].

The peaks at 2917 and 2850 cm^{-1} corresponded to the symmetric and asymmetric stretching vibrations of CH_2 and CH_3, respectively, belonging to the lipid chains or protein terminal groups. The peaks of bending vibrations of CH_2 and CH_3 groups of lipids appear at 1450 and 1374 cm^{-1}, respectively [15].

4.2. The Effect of pH on the Effectiveness of Dye Adsorption onto MM and ME

BV10 adsorption onto MM and ME was the highest at pH 3 and decreased as the pH increased, with the worst adsorption at pH 11. We noted the greatest decrease in BV10 adsorption effectiveness from pH 3 to pH 4, with a sharp decline at pH 2 (Figure 3A). The high BV10 adsorption effectiveness at a low pH could be due to the presence of the carboxyl functional group in its structure. Despite the generally cationic nature, the carboxyl group of the dye can be easily ionised and generate a negative local charge ($–COOH + H_2O \rightarrow –COO^- + H_3O^+$). Due to this negative charge, the protonated functional groups of the tested adsorbents attract BV10 electrostatically at a low pH, thereby significantly aiding in its adsorption. The functional groups protonated at a low pH are presumably acetamide groups (derived from chitin) as well as amino groups (derived from chitin and protein structures). At pH > 3, the total positive charge on the MM and ME surface decreases, a phenomenon that is reflected in the weaker attraction of the ionised carboxyl group of BV10 and, consequently, less effective dye adsorption. At pH 2, a significant part of the carboxyl groups of BV10 remain non-ionised (–COOH), which results in their weaker interaction with the adsorbent surface and decreased adsorption. In addition, this decline in BV10 adsorption effectiveness at pH 2 could be due to a high concentration of chloride ions (Cl^-), which might compete with BV10 for the adsorption centres of MM and ME. Researchers have noted a similar effect of pH on BV10 adsorption effectiveness when assessing its adsorption on coconut shells [18], pumpkin seed shells [19], and green tea leaves [20].

BR46 showed markedly different adsorption. The intensity of its adsorption onto MM and ME was the lowest at pH 2 and increased up to pH 6; there was an effectiveness peak as the pH increased from 2 to 4. From pH 4 to 8, the BR46 adsorption effectiveness was similar and high (Figure 3B). Presumably, the formation of hydrogen bridges between amine groups of the dye and amide groups of the adsorbent is the underlying mechanism by which BR46 is adsorbed onto MM and ME. At a low pH, BR46 – which has a positive charge in an aqueous solution – is electrostatically repulsed from the positively charged surface of MM and ME, which strongly impairs its adsorption. The pH increase results in fewer protonated functional groups of the adsorbent, which boosts the BR46 adsorption effectiveness. Researchers have reported a similar effect of pH on BR46 adsorption

effectiveness in studies with activated carbon [21], cyclodextrin-based nanosponges [22], and spent coffee grains [20] used as adsorbents.

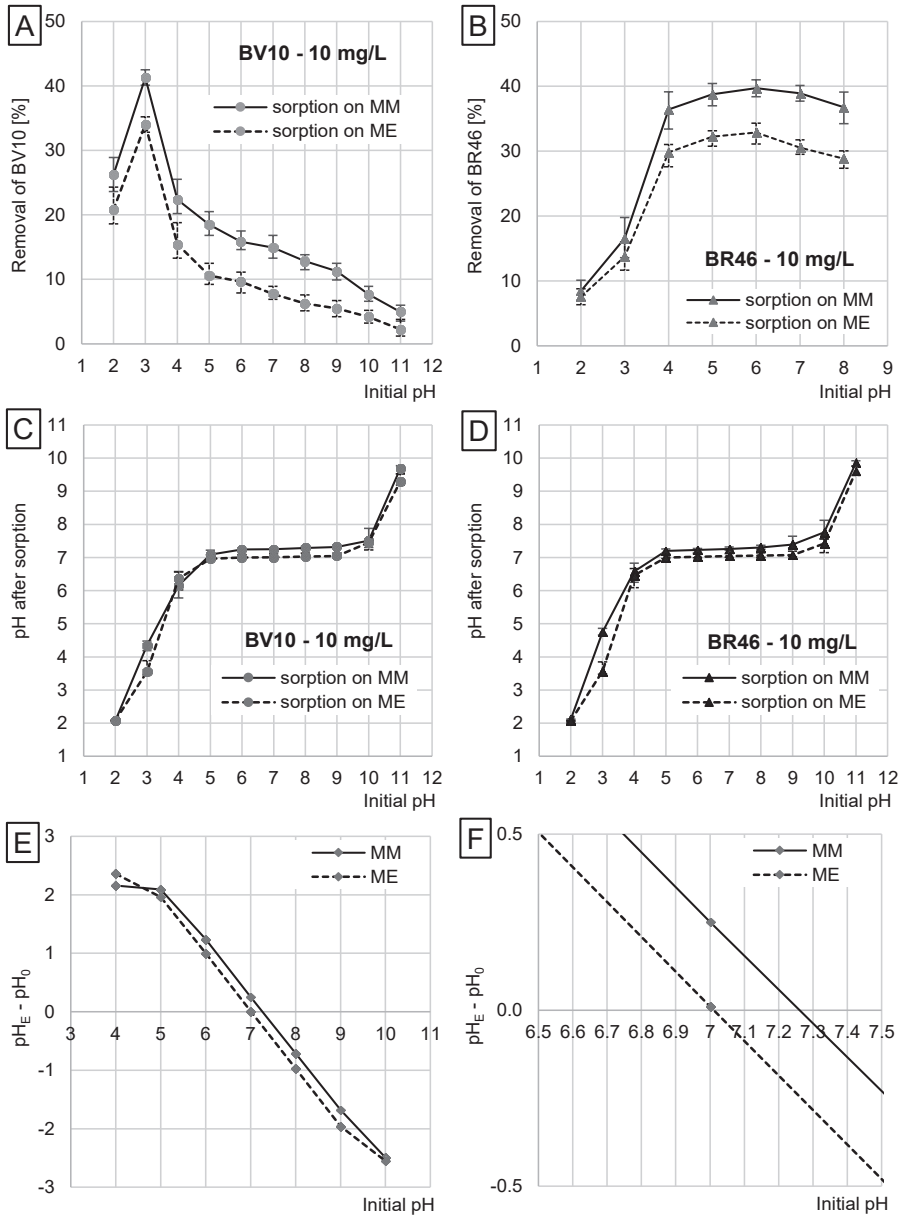

Figure 3. The effect of pH on the adsorption effectiveness of (A) Basic Violet 10 (BV10) and (B) Basic Red 46 (BR46) onto mealworm moults (MM) and mealworm exoskeletons (ME). The data represent the mean and range. The effect of MM and ME on the changes in the solution pH during dye adsorption of (C) BV10 and (D) BR46. (E and F) Determination of pH of the point of zero charge for MM and ME with the 'drift' method.

MM and ME modified the pH of the solutions during adsorption (Figure 3C and 3D). In the analyses conducted at the initial pH range of 5–10, the pH of the solutions ranged from 7.09 to 7.45 after dye adsorption onto MM and from 6.96 to 7.6 after dye adsorption onto ME. The adsorbents ability to neutralise solutions is because their functional groups could be ionised. At a pH close to neutral, most amine functional groups are in the protonated from ($–NH_3^+$), whereas most carboxyl groups (belonging to proteins) are in the deprotonated form ($–COO^–$). At a low pH, the functional groups of the adsorbents attached a proton from the hydronium ions present in the solution, which increased solution's pH:

$$-COO^- + H_3O^+ \rightarrow -COOH + H_2O;$$
$$-NH_2 + H_3O^+ \rightarrow -NH_3^+ + H_2O.$$

In turn, at a high pH, most of the functional groups are deprotonated, which results in the elimination of free hydroxyl ions from the solution and ultimately a decrease in the system's pH:

$$-NH_3^+ + OH^- \rightarrow -NH_2 + H_2O;$$
$$-COOH + OH^- \rightarrow -COO^- + H_2O.$$

Adsorptive materials always modify the pH to make it similar to pH_{PZC} – the pH at which the number of positive and negative charges on the adsorbent's surface are the same and the total electric charge of the material is null. The pH_{PZC} determined with the 'drift' method was 7.26 for MM and 7.02 for ME. The greater alkalinity of MM compared with ME is, presumably, due to a higher concentration of amine and amide functional groups capable of being protonated. The higher number of amine and amide functional groups in MM may be ultimately reflected in more adsorption centres and a higher adsorption capacity.

4.3. The Kinetics of BV10 and BR46 Adsorption onto MM and ME

The time needed to reach adsorption equilibrium on MM and ME depended on the dye concentration and in the case of BV10 also the adsorbent type. The adsorption of BV10 lasted for 180–210 min on MM and for 150–180 min on ME (Figure 4A and 4B). In turn, the adsorption of BR46 lasted for 120–150 min on both adsorbents (Figure 4C and 4D). Similar adsorption equilibrium times have been reported in studies evaluating BV10 adsorption onto activated carbon from jute fibre (220 min) [23], mushroom biomass (210 min) [24], coconut shells (180 min) [18], and carbonised coconut fibres (150 min) [25]. In the case of BR46, similar adsorption equilibrium times have been reported in experiments with chitin from MM (120 min) [6] and fir sawdust (120 min) [26].

The intensity of dye adsorption onto MM and ME was the highest within the first minutes of the process. After 30 min, the amount of BV10 and BR46 adsorbed on MM reached a minimum of 50% and 72% of q_e (where q_e is the amount of dye adsorbed at equilibrium), respectively. In the case of adsorption onto ME, these values were 63% and 61% of q_e for BV10 and BR46, respectively.

Generally, shorter dye adsorption times at higher dye concentrations could be due to the greater probability of collisions of adsorbate molecules with adsorption centres of the adsorbents, resulting in faster saturation of active sites and completion of the adsorption process. It is possible that it took less time for BV10 to reach adsorption equilibrium with ME compared with MM are because ME is less porous than MM. The experimental series with BR46 did not show a similar effect: the adsorption equilibrium times for MM and ME were the same. Presumably, the smaller BR46 and its stronger affinity for adsorption

centres compared with BV10 resulted in its more effective penetration of the adsorbent structure and equally fast occupation of available adsorption centres despite differences in their porosity. This also explains why BR46 reached adsorption equilibrium faster than BV10.

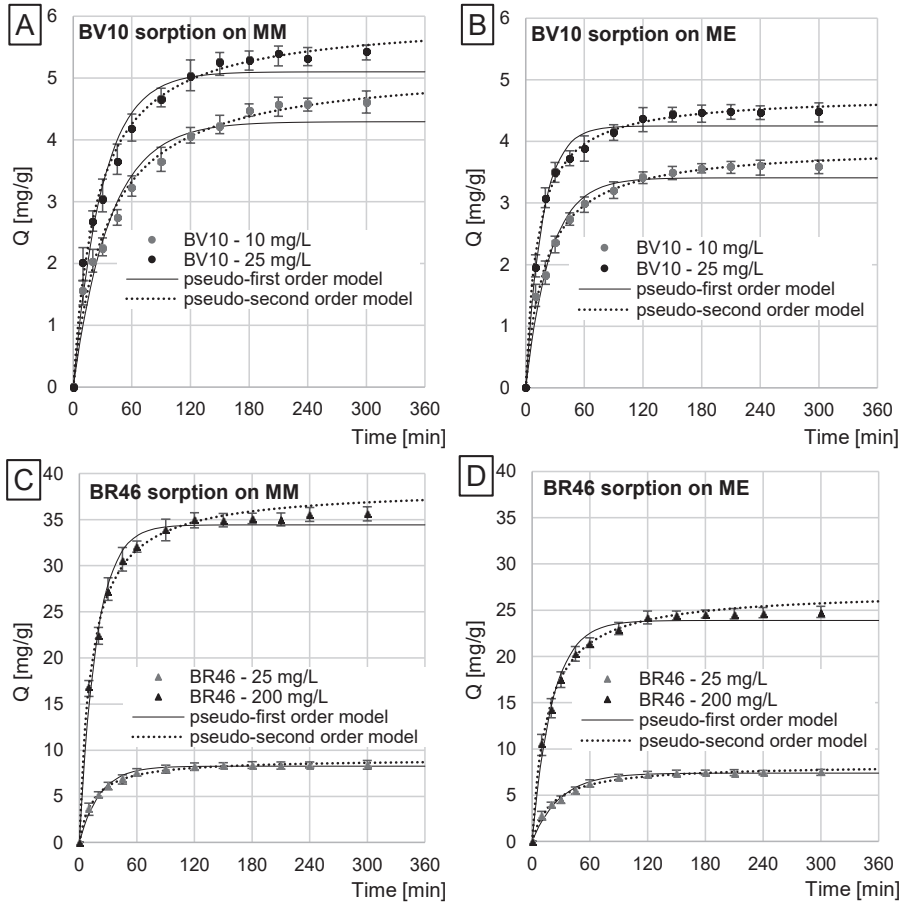

Figure 4. Changes in dye concentration over time: (A) Basic Violet 10 (BV10) adsorbed onto mealworm moults (MM), (B) BV10 adsorbed onto mealworm exoskeletons (ME), (C) Basic Red 46 (BR46) adsorbed onto MM, and D) BR46 adsorbed onto ME.

In each experimental series, the pseudo-second order model best fit the experimental data regardless of adsorbent type or dye concentration (Figure 4 and Table 1). This finding is typical for the adsorption of organic dyes onto biosorbents [19, 20]. The k_2 constant and q_e values are larger for dye adsorption onto MM than onto ME, a phenomenon that may be due to the greater specific surface area of MM.

Table 1. Kinetic parameters of adsorption of cationic dyes – Basic Violet 10 (BV10) and Basic Red 46 (BR46) – onto mealworm moults (MM) and mealworm exoskeletons (ME), determined from the pseudo-first order and pseudo-second order models (based on the average of three measurements).

Sorbent	Dye	Dye concentration [mg/L]	Pseudo–first order model			Pseudo–second order model			Exp. data
			k_1 [1/min]	$q_{e,cal.}$ [mg/g]	R^2	k^2 [g/mg*min]	$q_{e,cal.}$ [mg/g]	R^2	$q_{e,exp.}$ [mg/g]
MM	BV10	10	0.0266	4.29	0.9704	0.0057	5.20	0.9876	4.60
		25	0.0340	5.10	0.9779	0.0077	5.98	0.9964	5.40
	BR46	25	0.0469	8.26	0.9912	0.0069	9.05	0.9972	8.39
		200	0.0560	34.41	0.9938	0.0021	38.44	0.9972	35.60
ME	BV10	10	0.0401	3.41	0.9780	0.0131	3.92	0.9949	3.59
		25	0.0597	4.25	0.9870	0.0176	4.75	0.9964	4.47
	BR46	25	0.0345	7.38	0.9896	0.0087	8.27	0.9939	7.50
		200	0.0475	23.88	0.9906	0.0023	27.12	0.9993	22.70

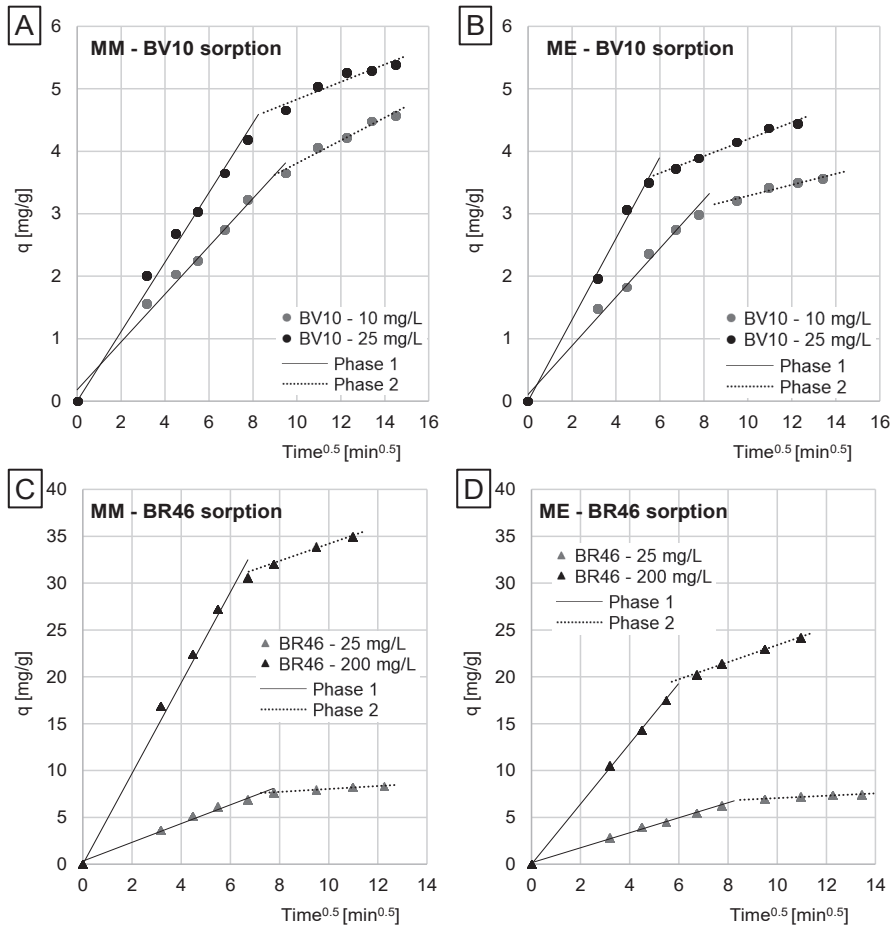

Figure 5. The intramolecular diffusion model of adsorption of (A) Basic Violet 10 (BV10) onto mealworm moults (MM), (B) BV10 onto mealworm exoskeletons (ME), (C) Basic Red 46 (BR46) onto MM, and (D) BR46 onto ME.

Table 2. Dye diffusion rate constants determined from the intramolecular diffusion model.

Sorbent	Dye	Dye conc. [mg/L]	Phase 1			Phase 2		
			k_{d1}* [*]	Duration [min]	R^2	k_{d2} [*]	Duration [min]	R^2
MM	BV10	10	0.3827	90	0.9869	0.1828	120	0.9705
		25	0.5569	60	0.9976	0.1405	120	0.9043
	BR46	25	0.9996	60	0.9847	0.1556	90	0.9706
		200	4.8412	45	0.9971	0.9178	75	0.9897
ME	BV10	10	0.3900	60	0.9891	0.0884	120	0.9336
		25	0.6514	30	0.9984	0.1356	120	0.9833
	BR46	25	0.8004	60	0.9952	0.1250	90	0.9454
		200	3.2213	30	0.9998	0.9120	90	0.9858

Note. * [mg/(g·min$^{0.5}$)]. BV10, Basic Violet 10; BR46, Basic Red 46; ME, mealworm exoskeletons; MM, mealworm moulds.

Analysis of the constants determined from the intramolecular diffusion model demonstrated that BV10 and BR46 adsorption onto MM and ME proceeded in two main phases (Figure 5 and Table 2). Presumably, in the first phase, dye molecules diffuse from the solution onto the adsorbent surface and attached to the most accessible adsorption centres. This phase shows high-intensity dye binding but is relatively short. The second phase begins when all active sites have been saturated on the adsorbent surface. Then, dye particles attach mainly to the adsorption centres located in deeper layers of the adsorbent. Due to strong competition between adsorbent molecules for free active sites and their potential difficulties in penetrating the adsorbent structure, the second phase of adsorption is significantly less effective and substantially longer than the first phase.

Table 3. Constants determined from the Langmuir 1, Langmuir 2, and Freundlich models.

Sorbent	Dye	Langmuir 1 model			Langmuir 2 model						Freundlich model		
		Q_{max} [mg/g]	K_c [l/mg]	R^2	Q_{max} [mg/g]	b_1 [mg/g]	K_1 [l/mg]	b_2 [mg/g]	K_2 [l/mg]	R^2	k	n	R^2
MM	BV10	6.44	0.407	0.979	6.44	2.16	0.407	4.28	0.407	0.979	2.39	0.32	0.862
	BR46	50.90	0.013	0.998	50.90	26.63	0.013	25.27	0.013	0.998	4.20	0.40	0.940
ME	BV10	5.56	0.260	0.992	5.56	2.79	0.260	2.77	0.260	0.992	1.62	0.38	0.917
	BR46	31.53	0.019	0.997	31.53	15.79	0.012	15.74	0.012	0.997	3.81	0.34	0.915

Note. BV10, Basic Violet 10; BR46, Basic Red 46; ME, mealworm exoskeletons; MM, mealworm moulds.

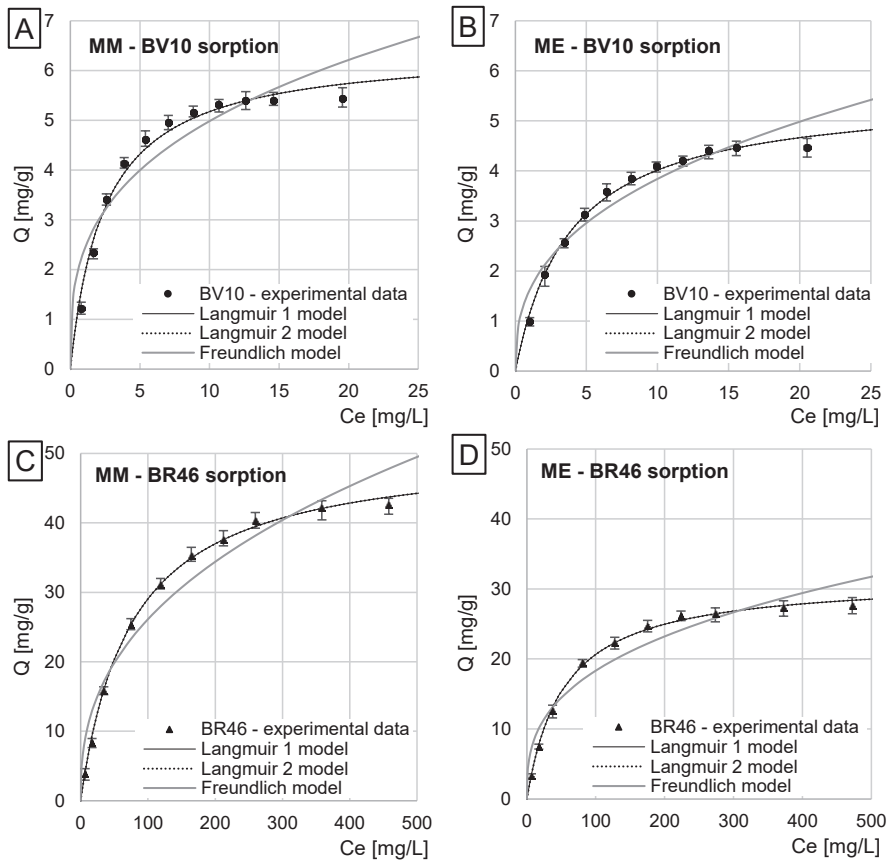

Figure 6. Adsorption isotherms of (A) Basic Violet 10 (BV10) onto mealworm moults (MM), (B) BV10 onto mealworm exoskeletons (ME), (C) Basic Red 46 (BR46) onto MM, and D) BR46 onto ME.

Compared with ME, MM had generally higher k_{d1} values and a longer duration of the first, key phase of adsorption (Table 2). These data confirm MM are more effective in the removal of BV10 and BR46 from aqueous solutions. In the experimental series with the same initial concentration of dyes (25 mg/l), the k_{d1} values determined for BR46 were higher than those for BV10, regardless of the adsorbent type, which suggests greater usability of the tested adsorbents for the removal of BR46.

4.4. The Maximum Adsorption Capacity of MM and ME

The Langmuir isotherms showed a better fit to the experimental data than the Freundlich isotherms in each experimental series (Figure 6 and Table 3). In addition, for both BV10 and BR46, the Q_{max} and K_C constant values determined from the Langmuir 1 model had the same numerical values as $Q_{max(b1+b2)}$ and K_1/K_2 constants determined from the Langmuir 2 model. The R^2 values were also identical (Table 3). These results suggest that only one type of adsorption centre played a key role during dye adsorption onto MM and ME. It is likely that protonated nitrogen atoms present in the amine and amide functional groups of adsorbents are the key adsorption centres for BV10, whereas non-ionised amide groups of MM and ME forming hydrogen bridges with tertiary amine groups of the dye are the key for BR46 adsorption.

Table 4. Comparison of the adsorption capacity of biosorbents and activated carbons for Basic Violet 10 (BV10) and Basic Red 46 (BR46).

Dye	Adsorbent	Adsorption capacity [mg/g]	Adsorption time [h]	pH of adsorption	Temp. [°C]	Source
BV10	Powdered coffee	2.50	3.0	2	19	[27]
	Coal–fired coconut fibre	2.60	2.5	6.5	25	[28]
	Chitosan (non–cross–linked granules)	2.94	24	6	25	[29]
	Chitin from the moults of mealworms	3.22	2.0	6	22	[6]
	Mango leaves (powder)	3.30	0.8	–	25	[30]
	Grapefruit peels	4.60	4.0	3	22	[31]
	Mealworm exoskeletons (ME)	**5.56**	**3.0**	**3**	**22**	**This work**
	Lemon peels	5.70	4.0	3	22	[31]
	Mealworm moults (MM)	**6.44**	**3.5**	**3**	**22**	**This work**
	Sugar cane fibre	10.4	–	–	25	[32]
	Sugar cane biomass	13.9	–	–	25	[33]
	Coconut fibre	14.9	1.5	9.2	32	[34]
	Cedar cones	17.2	8.0	5.0	25	[35]
	Banana peels	20.6	24	7.0	30	[36]
	Spent green tea leaves	26.7	4.0	3.0	22	[20]
	Activated carbon from jute fibre	28.0	3.6	8.0	–	[23]
	Coconut shells	28.5	3.0	3.0	22	[18]
	Palm–shell–based activated carbon	30.0	–	3.0	–	[37]
	Commercial activated carbon powder	72.5	24	4.0	25	[38]
BR46	Hen feathers	**4.1**	3.5	5.0	20	[39]
	Sawdust	**13.9**	–	–	20	[40]
	Wood sawdust	**19.2**	2.0	–	–	[41]
	Bone meal	**24.6**	1.5	6	20	[42]
	Nut Sawdust	**30.1**	–	7	20	[43]
	Mealworm exoskeletons (ME)	**31.5**	**3.0**	**6.0**	**22**	**This work**
	Paulownia tomentosa tree leaves	43.1	1.2	8.0	20	[44]
	Activated carbon ROW 08	45.0	1.0	8.0	20	[45]
	Mealworm moults (MM)	**50.9**	**2.5**	**6.0**	**22**	**This work**
	Chitin from the moults of mealworms	59.6	2.0	6.0	22	[6]
	Activated carbon from biomass of *Cerbera odollam*	**65.7**	1.5	7.0	20	[46]
	Granular activated carbon	**333.3**	< 1.0	8.0	–	[47]

Note. '–' means information not provided.

Q_{max} of MM was 6.44 mg/g for BV10 and 50.90 mg/g for BR46. Q_{max} for ME was lower: 5.56 and 31.53 mg/g for BV10 and BR46, respectively (Table 3). The $K_C/K_1/K_1$ constant values determined from the Langmuir model for dye adsorption onto MM were also higher than those determined for dye adsorption onto ME. This points to stronger affinity of the cationic dyes to functional centres of MM than to the active sites of ME. As mentioned in Section 4.2, this may be due to a higher number of amine and amide functional groups on the MM surface, which represent potential adsorption centres for the tested dyes. The higher dye adsorption effectiveness onto MM compared with ME could also stem from the greater porosity and specific surface area of MM (as mentioned in Section 4.3).

The differences noted in BV10 and BR46 adsorption effectiveness on the tested adsorbents could have also been due to the different functional groups of the dyes, which affect their adsorption mechanism and their affinity for the active centres of adsorbents. The carboxyl functional group of BV10, not typical of cationic dyes, generate a strong negative charge over a broad pH range. Presumably, the ionised $–COO^-$ groups partially neutralise the cationic character of the dye, thereby negatively affecting its ability to bind the adsorbent. The effectiveness of dye adsorption could also be strongly determined by molecular weight. The smaller size of BR46 compared with BV10 could facilitate its penetration to deeper layers of the adsorbent and its attachment to harder-to-access adsorption centres.

Table 4 summarises the adsorption capacities of various unconventional adsorbents towards BV10 and BR46.

The adsorption capacity of MM for BR46 is comparable to pure chitin from MM. In turn, the adsorption capacity of MM and ME for BV10 is approximately twofold higher than pure chitin from MM (Table 4). Presumably, the protein structures and mineral compounds of arthropod shells, which are usually removed during chitin extraction, have a comparable or even greater adsorption capacity than purified chitin. This suggests that the common processing of arthropod shells to obtain chitin adsorbents is not economical and may be perceived as a waste of material.

Compared with other unconventional adsorbents, the adsorption capacities of MM and ME for BV10 are rather low but comparable with adsorbents such as mango leaves and grapefruit skins. MM and ME exhibit a higher adsorption capacity for BR46 and may compete with adsorptive materials such as sawdust and some types of activated carbon (Table 4).

5. Conclusions

MM and ME can be successfully used as adsorbents to remove cationic dyes from aqueous solutions. The adsorption capacity of BV10 onto MM and ME was higher than onto adsorbents based on purified chitin or chitosan. The lower adsorption capacity of ME compared with MM for the two cationic dyes evaluated in this study might have been due to a lower content of both amine and amide functional groups and lower porosity of the adsorbent. The effectiveness of dye adsorption onto MM and ME was largely dependent on the solution's pH: BV10 adsorption was highest at pH 3 and BR46 adsorption was highest at pH 6.

MM and ME both modified the solution's pH during adsorption. The system always tended to reach the pH_{PZC}, 7.26 and 7.02 for MM and ME, respectively.

The dye adsorption equilibrium time onto MM was comparable for ME, whereas there were tangible differences in the adsorption times of BV10 and BR46. Generally, the adsorption equilibrium was reached earlier for the experimental series with BR46 (120–150 min) compared with BV10 (150–210 min), which may be attributed to the lower molecular weight of BR46 and its stronger affinity for the adsorption centres of the tested materials.

The binding of BV10 and BR46 onto MM and ME proceeded in two main phases that differed in intensity and duration. The first phase was crucial for the adsorption process. Although it was shorter than the second phase, it involved saturation of most adsorption centres available on the adsorbent's surface.

Only one type of active centre played a key role in the cationic dyes adsorbed onto MM and ME, which was indicated by identical values of $K_C/K_1/K_2$ and Q_{max} as well as R^2 determined from the Langmuir 1 and 2 isotherms. Presumably, the protonated nitrogen atoms present in the amine and amide functional groups of the adsorbents are the key adsorption centres for BV10, whereas non-ionised amide groups forming hydrogen bridges with tertiary amine groups of the dye are the key adsorption centres for BR46.

6. Acknowledgements

This study was financed under Project No. 29.610.023–300 of the University of Warmia and Mazury in Olsztyn, Poland.

7. References

[1] Rane A, Joshi SJ; (2021) Biodecolorization and biodegradation of dyes: a review. Open Biotechnol J 15, 97–108. **DOI:**10.2174/1874070702115010097

[2] Eltahan N, Kiwaan HA; (2022) Dyes, environmental impact and remediation by physical and chemical methods. SSRN Electronic J. **DOI:**10.2139/SSRN.4169103

[3] Al-Zawahreh K, Barral MT, Al-Degs Y, Paradelo R; (2021) Comparison of the sorption capacity of basic, acid, direct and reactive dyes by compost in batch conditions. J Environ Manage 294, 113005. **DOI:**10.1016/J.JENVMAN.2021.113005

[4] Algarni T saad, Al-Mohaimeed AM; (2022) Water purification by adsorption of pigments or pollutants via metaloxide. J King Saud Univ Sci 34, 102339. **DOI:**10.1016/J.JKSUS.2022.102339

[5] Deaconu M, Senin R; (2016) Adsorption decolorization technique of textile/leather - dye containing effluents. Int J Waste Resour 6, 2. **DOI:**10.4172/2252–5211.1000212

[6] Jóźwiak T, Filipkowska U, Bakuła T, Bralewska-Piotrowicz B, Karczmarczyk K, Gierszewska M, Olewnik-Kruszkowska E, Szyryńska N, Lewczuk B; (2023) The use of chitin from the molts of mealworm (Tenebrio molitor) for the removal of anionic and cationic dyes from aqueous solutions. Materials 16, 545. **DOI:**10.3390/MA16020545/S1

[7] Elieh-Ali-Komi D, Hamblin MR, Daniel E-A-K; (2016) Chitin and chitosan: production and application of versatile biomedical nanomaterials. Int J Adv Res 4, 411

[8] Sindermann D, Heidhues J, Kirchner S, Stadermann N, Kuhl A; (2021) Industrial processing technologies for insect larvae. J Insects Food Feed 7, 857–875. **DOI:**10.3920/JIFF2020.0103

[9] Triunfo M, Tafi E, Guarnieri A, Salvia R, Scieuzo C, Hahn T, Zibek S, Gagliardini A, Panariello L, Coltelli MB, De Bonis A, Falabella P; (2022) Characterization of chitin and chitosan derived from Hermetia illucens, a further step in a circular economy process. Sci Rep 12, 1–17. **DOI:**10.1038/s41598–022–10423–5

[10] Abidin NAZ, Kormin F, Abidin NAZ, Anuar NAFM, Bakar MFA; (2020) The potential of insects as alternative sources of chitin: an overview on the chemical method of extraction from various sources. Int J Mol Sci 21, 1–25. **DOI:**10.3390/IJMS21144978

[11] Song YS, Kim MW, Moon C, Seo DJ, Han YS, Jo YH, Noh MY, Park YK, Kim SA, Kim YW, Jung WJ; (2018) Extraction of chitin and chitosan from larval exuvium

and whole body of edible mealworm, Tenebrio molitor. Entomol Res 48, 227–233. **DOI:**10.1111/1748–5967.12304

[12] Mendez-Alpuche AA, Ríos-Soberanis CR, Rodriguez-Laviada J, Perez-Pacheco E, Zaldivar-Rae JA; (2020) Physicochemical comparison of chitin extracted from horseshoe crab (Limulus polyphemus) exoskeleton and exuviae. ChemistrySelect 5, 11745–11752. **DOI:**10.1002/SLCT.202000085

[13] Dahmane EM, Taourirte M, Eladlani N, Rhazi M; (2014) Extraction and characterization of chitin and chitosan from Parapenaeus longirostris from Moroccan local sources. Int J Polym Anal Charac 19, 342–351. **DOI:**10.1080/1023666X.2014.902577

[14] Negrea P, Cauni A, Kasapsaraçoğlu I, Butnariu M; (2015) The study of infrared spectrum of chitin and chitosan extract as potential sources of biomass. Dig J Nanomater Biostruct 10, 1129–1138

[15] Lozano M, Rodríguez-Ulibarri P, Echeverría JC, Beruete M, Sorolla M, Beriain MJ; (2017) Mid-infrared spectroscopy (MIR) for simultaneous determination of fat and protein content in meat of several animal species. Food Anal Methods 10, 3462–3470. **DOI:**10.1007/S12161–017–0879–1

[16] Kaya M, Sargin I, Aylanc V, Tomruk MN, Gevrek S, Karatoprak I, Colak N, Sak YG, Bulut E; (2016) Comparison of bovine serum albumin adsorption capacities of α-chitin isolated from an insect and β-chitin from cuttlebone. J Indust Eng Chem 38, 146–156. **DOI:**10.1016/J.JIEC.2016.04.015

[17] Bölgen N, Demir D, Öfkeli F, Ceylan S; (2016) Extraction and characterization of chitin and chitosan from blue crab and synthesis of chitosan cryogel scaffolds. J Turk Chem Soc A Chem 3, 131–144. **DOI:**10.18596/JOTCSA.00634

[18] Józwiak T, Filipkowska U, Bugajska P, Kalkowski T; (2018) The use of coconut shells for the removal of dyes from aqueous solutions. J Ecol Eng 19, 129–135. **DOI:**10.12911/22998993/89672

[19] Kowalkowska A, Jóźwiak T; (2019) Utilization of pumpkin (Cucurbita pepo) seed husks as a low-cost sorbent for removing anionic and cationic dyes from aqueous solutions. Desalination Water Treat 171, 397–407. **DOI:**10.5004/DWT.2019.24761

[20] Jóźwiak T, Filipkowska U, Struk-Sokołowska J, Bryszewski K, Trzciński K, Kuźma J, Ślimkowska M; (2021) The use of spent coffee grounds and spent green tea leaves for the removal of cationic dyes from aqueous solutions. Sci Rep 11, 1–12. **DOI:**10.1038/s41598–021–89095–6

[21] Akkari I, Graba Z, Bezzi N, Vithanage M, Kaci MM; (2022) New insights into the effective removal of Basic Red 46 onto activated carbon produced from pomegranate peels. Biomass Convers Biorefin 1, 1–14. **DOI:**10.1007/S13399–022–03401–4/TABLES/6

[22] Li L, Liu H, Li W, Liu K, Tang T, Liu J, Jiang W; (2020) One-step synthesis of an environment-friendly cyclodextrin-based nanosponge and its applications for the removal of dyestuff from aqueous solutions. Res Chem Intermed 46, 1715–1734. **DOI:**10.1007/S11164–019–04059-W/TABLES/3

[23] Porkodi K, Vasanth Kumar K; (2007) Equilibrium, kinetics and mechanism modeling and simulation of basic and acid dyes sorption onto jute fiber carbon: eosin yellow, malachite green and crystal violet single component systems. J Hazard Mater 143, 311–327. **DOI:**10.1016/J.JHAZMAT.2006.09.029

[24] Jóźwiak T, Filipkowska U, Pyko B; (2022) Use of waste biomass of common mushroom (Agaricus bisporus) as a sorbent for the removal of Reactive Black 5 and Basic Violet 10 dyes from aqueous solutions. Desalination Water Treat 272, 303–315. **DOI:**10.5004/DWT.2022.28843

[25] Hamzeh Y, Ashori A, Azadeh E, Abdulkhani A; (2012) Removal of Acid Orange 7 and Remazol Black 5 reactive dyes from aqueous solutions using a novel biosorbent. Mater Sci Eng C 32, 1394–1400. **DOI:**10.1016/J.MSEC.2012.04.015

[26] Shukla A, Zhang YH, Dubey P, Margrave JL, Shukla SS; (2002) The role of sawdust in the removal of unwanted materials from water. J Hazard Mater 95, 137–152. **DOI:**10.1016/S0304–3894(02)00089–4

[27] Shen K, Gondal MA; (2017) Removal of hazardous rhodamine dye from water by adsorption onto exhausted coffee ground. J Saudi Chem Soc 21, S120-S127. **DOI:**10.1016/J.JSCS.2013.11.005

[28] Namasivayam C, Dinesh Kumar M, Selvi K, Ashruffunissa Begum R, Vanathi T, Yamuna RT; (2001) 'Waste' coir pith—a potential biomass for the treatment of dyeing wastewaters. Biomass Bioenergy 21, 477–483. **DOI:**10.1016/S0961–9534(01)00052–6

[29] Jóźwiak T, Filipkowska U, Filipkowska M; (2022) Effect of ionic and covalent crosslinking of hydrogel chitosan beads on the adsorption efficiency of Basic Violet 10 and Basic Green 4 dyes from aqueous solutions. Prog Chem Appl Chitin Deriv 27, 116–134. **DOI:**10.15259/PCACD.27.009

[30] Khan TA, Sharma S, Ali I; (2011) Adsorption of Rhodamine B dye from aqueous solution onto acid activated mango (Magnifera indica) leaf powder: equilibrium, kinetic and thermodynamic studies. J Toxicol Environ Health Sci 3, 286–297. **DOI:**10.5897/JTEHS.9000003

[31] Jóźwiak T, Filipkowska U, Zajko P; (2019) Use of citrus fruit peels (grapefruit, mandarin, orange, and lemon) as sorbents for the removal of basic violet 10 and basic red 46 from aqueous solutions. Desalination Water Treat 163, 385–397. **DOI:**10.5004/DWT.2019.24453

[32] Parab H, Sudersanan M, Shenoy N, et al; (2009) Use of agro-industrial wastes for removal of basic dyes from aqueous solutions. Clean 37, 963–969. **DOI:**10.1002/CLEN.200900158

[33] Ho YS, Chiu WT, Wang CC; (2005) Regression analysis for the sorption isotherms of basic dyes on sugarcane dust. Bioresour Technol 96, 1285–1291. **DOI:**10.1016/J.BIORTECH.2004.10.021

[34] Sureshkumar M V., Namasivayam C; (2008) Adsorption behavior of Direct Red 12B and Rhodamine B from water onto surfactant-modified coconut coir pith. Colloids Surf A Physicochem Eng Asp 317, 277–283. **DOI:**10.1016/J.COLSURFA.2007.10.026

[35] Zamouche M, Hamdaoui O; (2012) Sorption of Rhodamine B by cedar cone: effect of pH and ionic strength. Energy Proc 18, 1228–1239. **DOI:**10.1016/J.EGYPRO.2012.05.138

[36] Annadurai G, Juang RS, Lee DJ; (2002) Use of cellulose-based wastes for adsorption of dyes from aqueous solutions. J Hazard Mater 92, 263–274. **DOI:**10.1016/S0304–3894(02)00017–1

[37] Mohammadi M, Hassani AJ, Mohamed AR, Najafpour GD; (2010) Removal of Rhodamine B from aqueous solution using palm shell-based activated carbon: adsorption and kinetic studies. J Chem Eng Data 55, 5777–5785. **DOI:**10.1021/JE100730A

[38] Filipkowska U, Jóźwiak T, Szymczyk P, Kuczajowska-Zadrożna M; (2017) The use of active carbon immobilised on chitosan beads for RB5 and BV10 dye removal from aqueous solutions. Prog Chem Appl Chitin Deriv 22, 14–26. **DOI:**10.15259/PCACD.22.02

[39] Jóźwiak T, Filipkowska U, Marciniak P; (2021) Use of hen feathers to remove reactive black 5 and basic red 46 from aqueous solutions. Desalination Water Treat 232, 129–139. **DOI:**10.5004/DWT.2021.27513
[40] Doltabadi M, Alidadi H, Davoudi M; (2016) Comparative study of cationic and anionic dye removal from aqueous solutions using sawdust-based adsorbent. Environ Prog Sustain Energy 4, 1078–1090. **DOI:**10.1002/EP.12334
[41] Laasri L, Elamrani MK, Cherkaoui O; (2007) Removal of two cationic dyes from a textile effluent by filtration-adsorption on wood sawdust. Env Sci Poll Res Int 14, 237–240. **DOI:**10.1065/espr2006.08.331
[42] El Haddad M, Rachid M, Slimani R, Nabil S, Ridaoui M, Lazar S; (2012) Adsorptive removal of a cationic dye -Basic Red 46 -from aqueous solutions using animal bone meal. J Eng Stud Res 18. 43–52.
[43] Yeddou N, Bensmaili A; (2005) Kinetic models for the sorption of dye from aqueous solution by clay-wood sawdust mixture. Desalination 185, 499–508. **DOI:**10.1016/J.DESAL.2005.04.053
[44] Deniz F, Saygideger SD; (2011) Removal of a hazardous azo dye (Basic Red 46) from aqueous solution by princess tree leaf. Desalination 268, 6–11. **DOI:**10.1016/J.DESAL.2010.09.043
[45] Madeła M, Krzemińska D, Neczaj E; (2014) Wpływ procesu Fentona na skuteczność usuwania zanieczyszczeń ze ścieków przemysłowych na węglach aktywnych. Technologia Wody 37, 46–50.
[46] Azmi NAI, Zainudin NF, Ali UFM; (2015) Adsorption of basic Red 46 using sea mango (Cerbera odollam) based activated carbon. AIP Conf Proc 1660, 070068. **DOI:**10.1063/1.4915786
[47] Abdul Halim HN, Mee KLK; (2011) Adsorption of Basic Red 46 by granular activated carbon in a fixed- bed column. Int Conf Environ Ind Innov 12, 263–267.